Molecular Beam Chemistry: Formation of Benzene and Other Higher Hydrocarbons from Small Alkanes and Alkenes in a Catalytic Supersonic Nozzle

Lina Shebaro,[†] Sameer R. Bhalotra, and Dudley Herschbach*

Department of Chemistry and Chemical Biology, Harvard University, 12 Oxford Street, Cambridge, Massachusetts 02138

Received: March 17, 1997; In Final Form: May 20, 1997[⊗]

Large yields of higher hydrocarbons are produced by flowing C2, C3, or C4 alkanes or alkenes, typically at 80 Torr, 1000 °C, and 10 ms contact time, through a supersonic nozzle made of nickel or molybdenum. In the mass spectra of the products, C_nH_m, the most prominent peaks (extending to $n = 12$) contain even numbers of carbon atoms, but there are also substantial peaks with odd carbon atom numbers. The largest peaks have $m \sim n$ hydrogen atoms, but many others also appear. For $n = 6$ the mass spectrum indicates benzene is essentially the sole product. The total conversion of the parent beam is roughly 40−60%, of which typically 15−25% is benzene; the yields increase as C2 → C4 and are appreciably higher for alkenes. Under the same conditions, methane does not form higher hydrocarbons. Experiments with mixtures of CD_4 and C_2H_6 show, however, that D atoms from methane pervade the higher hydrocarbon products.

1. Introduction

Long ago, in his classic work on the interaction of hydrogen with tungsten, Langmuir described a prototypical heterogeneous−homogeneous reaction, in which radicals formed by dissociative chemisorption desorb into the gas phase and react there.[1] In modern times, the role of such surface-generated gas-phase radicals in catalytic reactions has been directly demonstrated in several processes,[2] and suspected or postulated in many more. Here we report experiments indicating that in a supersonic molecular beam such a mechanism offers a remarkably facile means to produce higher hydrocarbons, including numerous free radicals and benzene, from small alkanes or alkenes.

Supersonic molecular beams have long offered a versatile tool for both collision and spectroscopic experiments.[3] The markedly nonequilibrium character of the gas flow produces drastic cooling of molecular motion. This also enables generating beams of chemical species that are not feasible to study in an equilibrium gas, including a host of van der Waals adducts[4] and atomic and molecular clusters.[5] Several special nozzle designs have been developed to handle refractory,[6] delicate,[7] or reactive species, particularly organic free radicals.[8] Pulsed nozzles have proven very effective,[9] especially when coupled with vaporization by laser ablation of solids into the gas flow;[10] this led to the discovery in carbon clusters of fullerene molecules. In the present work, we use a simple nozzle fashioned from a catalytic metal.[11] Precursor radicals, formed on the hot metal surface, evidently are swept off into the flowing gas and induce chain reactions. The traditional catalytic role, merely accelerating the attainment of equilibrium, thereby can be much augmented by exploiting the markedly nonequilibrium environment provided by a supersonic expansion.

On simply flowing ethane or ethylene gas through such a nozzle, at typically 80 Torr and 1000 °C, with 10 ms contact time, we find that roughly 40% is converted to higher hydrocarbons, C_nH_m. These hydrocarbons contain from $n = 3$ to 12 carbon atoms and a range of hydrogen atoms, mostly equal to or near the number of carbon atoms ($m \sim n$). Although our mass spectrometric detection cannot be entirely definitive, the C_6H_6 product appears to be solely benzene; its yield is typically about 15%. When the reactant gas is a C3 or C4 alkane or alkene, the overall conversion and benzene yields are appreciably higher. At present, we know of no other single-pass process that gives such high conversion.

In contrast to our results, in pyrolysis of ethane in glass reactors (up to ∼800 °C and 1 atm, without catalyst) the initial, short-time products contain only traces of higher hydrocarbons.[12] Studies of dissociative chemisorption of methane[13] and ethane[14] on nickel under UHV conditions or in static gas systems (at ∼500 °C and 1 Torr) find the yield of benzene and other higher hydrocarbons is of the order of 1% or less. For comparable conditions (∼1000 °C and 80 Torr), ethane in a static system would reach thermodynamic equilibrium and decompose entirely, to form carbon on the metal surface and hydrogen in the gas phase. The facile formation of higher hydrocarbons in a supersonic flow thus exemplifies the use of kinetics to evade thermodynamic limitations. As in other recent work in pursuit of kinetic control of surface chemistry,[15] the key requisite is a way to restrict the interaction of reactive intermediates or products with the surface.

An efficient means to generate intense beams of hydrocarbon species can serve also to facilitate laboratory studies of radicals involved in gas-phase carbon chemistry.[16] For instance, in our beams, the flux of C_3H_3, C_4H_2, and C_4H_4 species are typically all well above 10^{17}/s, about 50-fold higher than other molecular beam sources for such species. Since our beams contain many components, they are suitable only when that is not a handicap, as in molecular beam microwave spectroscopy. However, such studies of hydrocarbon radicals have now become very active because these radicals not only appear in many familiar thermal and photochemical processes but also in the interstellar medium.[17] Microwave radioastronomy has detected C_nH with $n = 1-11$ and C_nH_2 with $n = 2-6$. Searches for other C_nH_m species would be greatly aided if their spectra can first be observed in laboratory experiments. Impetus has come from recent evidence that neutral−neutral reactions of carbon atoms with unsaturated hydrocarbons are important in some circumstellar envelopes.[18]

2. Apparatus and Experimental Conditions

Figure 1 shows a schematic view of the molecular beam apparatus. The source chamber contains the supersonic nozzle

[†] Also at Merkert Chemistry Center, Boston College, Chestnut Hill, MA 02167.

[⊗] Abstract published in *Advance ACS Abstracts,* July 15, 1997.

S1089-5639(97)00956-0 CCC: $14.00

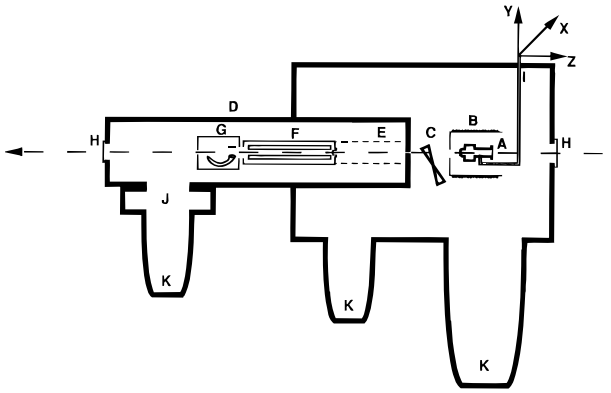

Figure 1. Schematic diagram of molecular beam apparatus: (A) supersonic nozzle; (B) water-cooled shield; (C) beam chopper; (D) mass spectrometer chamber; (E) ionizer and ion optics; (F) quadrupole mass filter; (G) electron multiplier; (H) windows used for alignment; (I) gas inlet and kinematic translation device; (J) liquid nitrogen baffle; (K) diffusion pumps.

assembly, much of which is enclosed in a cylindrical water-cooled can which serves as a heat sink to shield the rest of the apparatus. It is pumped by an unbaffled 10 in. diffusion pump and baffled 6 in. pump (Varian VHS-10 and VHS-6), both backed at the foreline by a 50 cfm mechanical pump (Alcatel 2063 CP+). The detector chamber contains an electron bombardment ionizer, ion optics, quadrupole mass filter, and electron multiplier. It is pumped by a liquid nitrogen cryotrap (Varian 362-6) augmented by a 6 in. diffusion pump (VHS-6) backed by an 18 cfm mechanical pump (Welch 1397). Other than its augmented pumping and the nozzle assembly, most features of the apparatus resemble those for recent studies in this laboratory.[7]

The molecular beam emerging from the nozzle is modulated by a mechanical chopper wheel at 200 Hz. The beam then enters the detection chamber via a 5 mm diameter aperture and traverses an electron bombardment ionizer. The bombarding energy was usually 31 eV. Guided by focusing lenses, the ions formed go into a quadrupole mass filter and are detected by an electron multiplier which feeds a lock-in amplifier. With the electron bombarder off, no ions were observed even at the highest nozzle temperatures used.

In typical experiments, the reactant gas enters the nozzle at a pressure of about 20 Torr at room temperature, and mass spectra of the emergent beam are recorded as the nozzle temperature is raised. The ambient pressure within the nozzle rises to about 85 Torr at the maximum temperature used, 1100 °C. The flow rate through the nozzle is of the order of 10^{19} molecules/s, and the residence time for a molecule in the hot nozzle before emerging from the orifice is about 10 ms. The background pressure in the source chamber was usually in the low 10^{-6} Torr range, and in the detection chamber in the low 10^{-7} range. The reactant gases examined (supplied by Matheson, >99% purity) were methane, ethane, ethylene, mixtures of methane or deuterated methane with ethane, and propane, propene, isobutane and isobutene.

Supersonic Nozzle. Figure 2 is a scale drawing of the nozzle. For most of the experiments reported here, the snout of the nozzle was a hollow nickel cylinder 2 cm long, with walls 5 mm thick, and a 4 mm internal diameter. The exit orifice was 0.35 mm in diameter, 0.38 mm deep. Heating coils made of 0.5 mm diameter tantalum wire wound about alumina rods 4 mm in diameter occupy 11 of 12 channels located around the nozzle perimeter; a tungsten/rhenium thermocouple is in the other channel. For consistency with data compiled elsewhere,[19] we report nominal temperatures measured by this thermocouple;

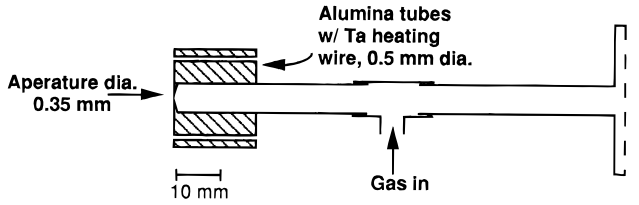

Figure 2. Cut-away view of supersonic nozzle, drawn to scale. Nozzle body of nickel or molybdenum, with snout containing heaters and a tubular extension joined via a Swagelok coupling to a gas feed tube of thin-walled stainless steel. The Swagelok coupling permits easy detachment and a widow (at right) aids alignment.

however, calibration runs with a similar thermocouple placed in the nozzle barrel show these nominal values are lower by about 6% than the actual temperature within the barrel. The maximum operating temperature of the nozzle is about 1200 °C. A tubular extension at the rear of the nozzle, with internal diameter 4 mm and wall thickness 2.5 mm, is linked via a Swagelok coupling to a stainless steel gas inlet tube, with internal diameter 4 mm and wall thickness 1.5 mm. The inlet tube is suspended from a kinematic mount and equipped with a viewing window to enable precise alignment of the nozzle.

With use, there occurs a gradual decline in the efficacy of the nozzle in producing higher hydrocarbons, although this does not appear to affect the relative amounts of the different products. The overall yields obtained with a freshly machined nickel nozzle decrease noticeably after many cycles of heating and cooling. This is referred to as the "weary nozzle syndrome." Typically, a new nozzle works well for about 50 h, but the product yield declines markedly after 70 h. A useful lifetime of about 100 h was attained by cleaning the nozzle regularly. This involves removing the viewing window (Figure 2), inserting and twisting a drill bit to remove carbonaceous deposits, followed by soaking in acetone and ultrasonic cleaning. This procedure was adequate for runs with ethane and ethylene. Attempts to use acetylene were not pursued because the nozzle quickly clogged with soot.

Several variant nozzles were also tried. In runs with ethane and ethylene, we found a molybdenum nozzle gave the same products as nickel, with equally high yield; unfortunately, brittleness made this nozzle impractical. With a stainless steel (304) nozzle, we observed a modest yield of some products (n = 3, 4, 6), but with an iron nozzle (possibly oxidized) we saw none. We also examined the effect of varying the surface area within a nickel nozzle. For our standard version (Figure 2), the internal area is 2.2 cm^2. This was more than doubled by installing a nickel coil, but that made no noticeable difference in the yield of products. Some preliminary results were obtained with a nozzle that has a detachable nickel "button" containing the exit aperture mounted on an iron body. Although in this design the nickel surface area is only 0.15 cm^2, the yield of higher hydrocarbons was if anything slightly enhanced.

3. Mass Spectra of Reactants and Products

The information provided by our experiments stems chiefly from comparing mass spectra obtained with the nozzle cool or hot. After examining results for ethane and ethylene, including the temperature dependence and concomitant reactant spectra, we consider C3 and C4 reactants, which produce larger yields of higher hydrocarbons, and then describe results for methane and mixtures of methane with ethane.

Ethane and Ethylene. With either ethane or ethylene, when the nozzle temperature reaches about 800 °C, product peaks appear in the mass spectra. With further rise in temperature,

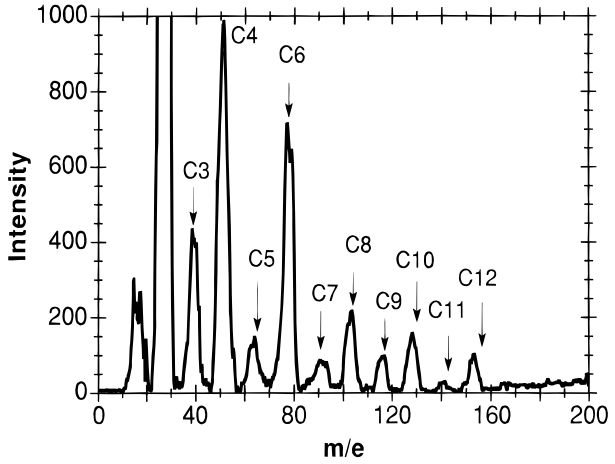

Figure 3. Typical low resolution mass spectrum of products from ethane reactant (1060 °C, 85 Torr) in Ni nozzle. Electron bombardment energy was 23 eV. The product peaks for C_nH_m are labeled by n, the number of carbon atoms. Arrows indicate masses for $m = n$ (located at $n \times 13$ mass units); thus $m \approx n$ up to $n = 8$ but the most probable m is lower by 1−3 units for higher n.

these grow markedly stronger and extend to higher masses. Figure 3 shows a typical low resolution mass spectrum. By 1000 °C, product peaks for C_nH_m with up to $n = 12$ carbon atoms are readily observed. The intensity distribution among the product peaks varies considerably with nozzle conditions (as usual for supersonic beams). However, the peaks for even n are consistently stronger than neighboring peaks for odd n, especially in the range $n = 3-6$.

For each n at higher resolution, as illustrated in Figure 4, subpeaks appear corresponding to various numbers of hydrogen atoms; the strongest of these usually have $m = n$ but in several cases others with 0 to $2n$ also occur. Some of the mass peaks may be due solely or partly to fragmentation on electron bombardment. However, as judged from comparing intensity variations over a wide range of nozzle conditions and bombarding voltage (26−70 eV), at least for the more prominent peaks this seems not to be the case. The principal mass peak in the $n = 3$ region corresponds to C_3H_3. This is likely the propargyl radical, $H-C\equiv C-CH_2$, a commonly postulated intermediate in combustion and pyrolysis processes.[20] The peaks nominally corresponding to C_3H_m with $n = 2$, 4, 5, 6, and 8 all also appear to arise chiefly from primary products rather than fragmentation. In the $n = 4$ region, peaks with $m = 2$, 3, and 4 are comparable; in the $n = 5$ region, peaks with $m = 3$, 5, and 6.

In the $n = 6$ region, shown in Figure 5, the mass spectrum indicates the major and probably sole six-carbon product is benzene. There are several aliphatic C_6H_6 isomers with fragmentation patterns similar in several respects to that of benzene: all have a strong 78 peak and weak 77, as well as 63 and 50−52 peaks that in our spectra are obscured by other products.[21] However, a fragment at mass 76 appears for benzene which does not occur for any of the aliphatic isomers. The intensity ratio 76/78 is consistent with benzene as the product, so offers evidence that the other isomers are indeed absent (as otherwise the ratio would be lower). A definitive analysis may be feasible by means of gas chromatography/mass spectrometry. Studies of flame systems have shown that above 400 °C the aliphatic isomers readily rearrange to form benzene as the predominant C_6H_6 product.[22]

Product Yields. From the ratio of the area under the mass peak(s) for the product(s) to that for ethane reactant, we estimate that above ∼1000 °C roughly 40% of the parent beam reacts and the benzene yield is typically 5−10% for a weary nozzle,

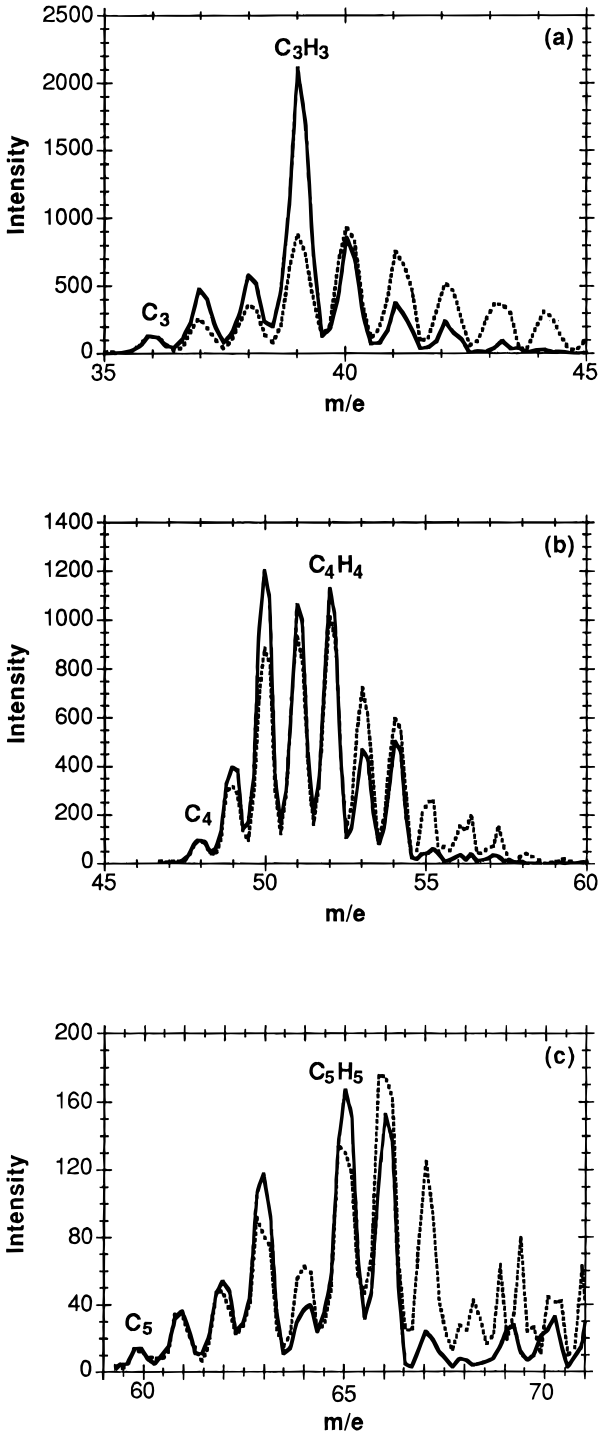

Figure 4. High-resolution mass spectra of $n = 3$, 4, 5 regions, for products from ethane at 1068 °C and 85 Torr (full traces) compared with equimolar mixture of CD_4 and C_2H_6 at 1068 °C and total 85 Torr (dashed traces, normalized to full traces at the C_n peak). Note variation with n of ordinate scale.

15% for a fresh one. These are nominal estimates, since no allowance is made for variations in detection efficiency of the mass spectrometer or possible mass separation effects in the supersonic expansion. Both effects would tend to overestimate the size of the mass peaks seen for the heavier products. However, we found a consistent estimate for the conversion of the reactant gas in another way, not involving areas of the product peaks. This employed an ethane beam to which ∼1% argon had been added. By comparing the intensities of the C2 and Ar mass peaks with the beam cool (∼30 °C) or hot (∼1000 °C), we obtained an estimate for the attenuation of the ethane

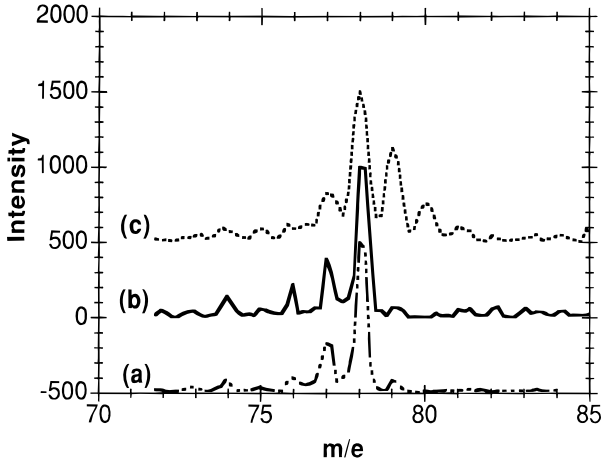

Figure 5. High-resolution mass spectrum of $n = 6$ region, for (a) molecular beam of benzene at 31 °C and 25 Torr, compared with product from (b) ethane at 1068 °C and 85 Torr and (c) equimolar mixture of CD_4 and C_2H_6 at 1068 °C and total 85 Torr. Ordinate scale pertains to (b); for (a) and (c) the height of mass 78 peak is normalized to (b) but baselines for the traces are shifted for clarity.

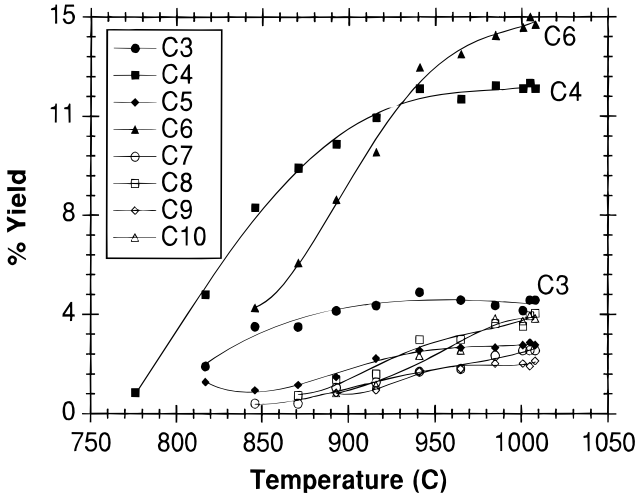

Figure 6. Temperature dependence of yield of higher hydrocarbons from ethane reacting in a Mo nozzle. At room temperature, the pressure of ethane was 20 Torr; as the nozzle was heated to 1010 °C, the pressure increased to 80 Torr. Yields are nominal, computed from ratio of area of mass peak to total of areas of all peaks from reactant as well as products.

beam due to reaction; this agreed within 5% with that derived from areas of the product peaks.

Although the array of product mass peaks were identical for ethylene and ethane, at a given source pressure and temperature the overall conversion of the parent beam and the benzene yield were both usually about 15% higher for ethylene.

Temperature Dependence. Figure 6 illustrates the variation in yield with nozzle temperature, for the case of ethane as reactant and a Mo nozzle. As the temperature is raised, the $n = 4$ and $n = 6$ product peaks increase most strongly and eventually $n = 6$ becomes most prominent. Qualitatively similar behavior was found for all the reactant gases examined (other than methane), for both Ni and Mo nozzles. The yield of $n = 6$ attained on reaching ~1000 °C varies substantially, however, depending on the identity of the reactant gas (cf. Figure 9) and the nozzle condition (fresh or weary).

Reactant Spectra. Figure 7 compares the mass spectra of ethane and a CD_4/C_2H_6 mixture at low and high temperatures. The spectra for an ethane beam from an unheated nozzle (27 °C) displays a familiar fragmentation pattern, with a single

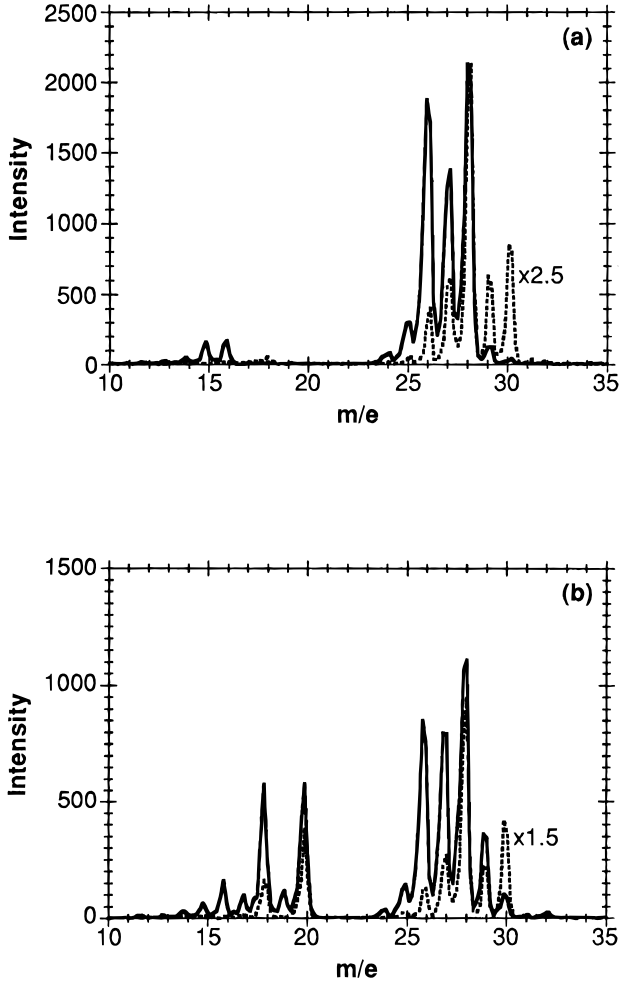

Figure 7. Mass spectra in C1, C2 region for (a) ethane and (b) CD_4/C_2H_6 mixture, comparing spectra for hot Ni nozzle (full curves, 1013 °C) with cool nozzle (dashed curves, 27 °C).

strong $C_2H_4^+$ peak (at $m/e = 28$) and four appreciable subsidiary peaks (26, 27, 29, 30) corresponding to $C_2H_2^+$...$C_2H_6^+$. However, for ethane from a hot nozzle (1013 °C), the subsidiary peaks (26, 27) for $C_2H_2^+$ and $C_2H_3^+$ have become strong, the other two weak (29, 30); also additional peaks appear (15,16) corresponding to CH_3^+ and CH_4^+. These features are consistent with formation of C_2H_4 and CH_4, since the observed mass peaks and their approximate relative intensities can all be accounted for by the fragmentation patterns for ethylene and methane. This suggests that, at least for the C1 and C2 regions, any free radical intermediates formed from the reactant gas do not appear in the emergent beam.

However, even for the Cl and C2 regions, the mass spectra obtained from the 1:1 CD_4/C_2H_6 mixture does provide evidence of radical intermediates. For a beam from an unheated nozzle, the mass spectrum shows, as expected, only peaks corresponding to the unreacted mixture. On heating, however, products involving both H and D atoms appear, as evident from new peaks (17, 19) and enhancements of other peaks (16, 29). These suggest that, in addition to D atoms, carbon-containing radicals derived from methane are probably involved to some extent in reactions within the nozzle.

C3 and C4 Alkanes and Alkenes. Figure 8 shows typical mass spectra for propane, propene, isobutane, and isobutene, obtained for runs using a Ni nozzle with the reactant gases at the same pressure and nozzle temperature, 60 Torr and 1035 °C. For both the C3 and C4 reactants, the mass spectra show extensive fragmentation, chiefly from loss of a methyl group.

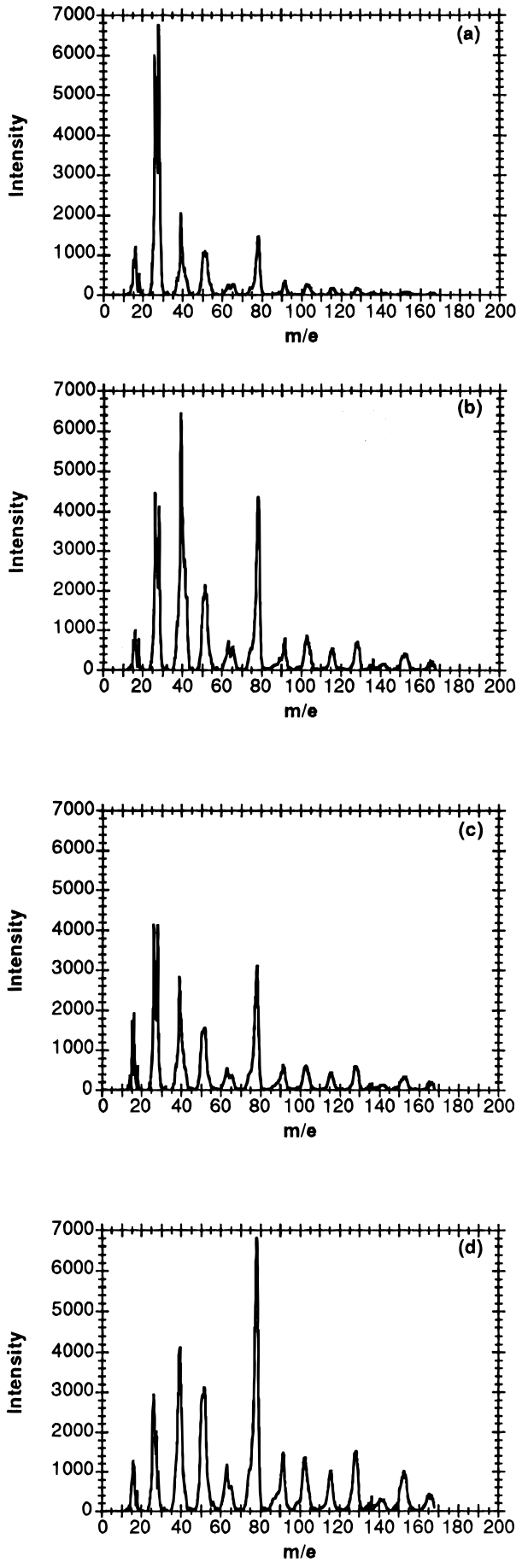

Figure 8. Mass spectra for reactants and products from (a) propane, (b) propene, (c) isobutane, and (d) isobutene reacting in Ni nozzle at 60 Torr and 1035 °C.

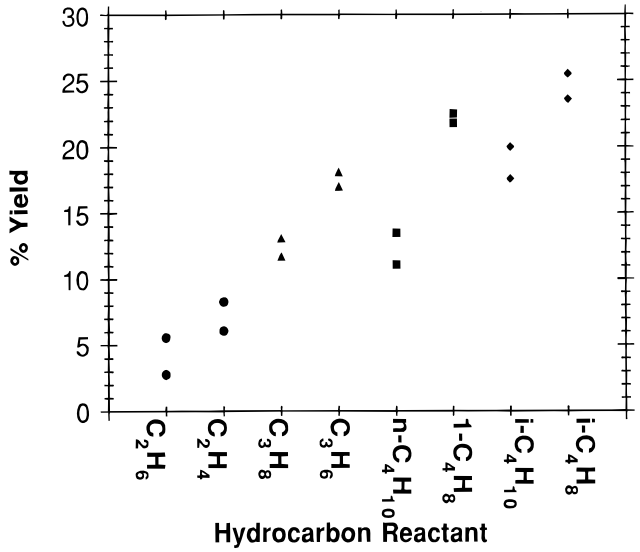

Figure 9. Comparison of yield of benzene for C2, C3, and C4 alkane and alkene reactants for Ni nozzle operated at 60 Torr and 1035 °C. Data points are shown for two sets of experiments.

The nominal yields of higher hydrocarbons therefore were evaluated by dividing the area under each C*n* peak by the total area under all reactant and product peaks, including those arising from the fragmentation of the reactant gas. The formation of higher hydrocarbons was found to increase substantially as the reactant gas was changed from C2 → C4, or for given *n* changed from alkane to alkene. Figure 9 compares the yield of benzene for the eight reactant gases examined. In this set of runs, it was lower than usual for ethane and ethylene, only ∼4−8% (perhaps because the Ni nozzle used for this set of runs was "weary" and the source pressure was somewhat low). However, the benzene yield climbed markedly for the larger reactant molecules, reaching for isobutene roughly 25%.

Methane and Mixtures. In contrast, under the same conditions methane gives no discernible higher hydrocarbons. This raised the question whether mixing ethane or ethylene with methane might supply reactive intermediates that would enable methane to contribute to the higher products. We made a series of runs, varying total gas pressure and temperature for three methane/ethane mixtures, with methane 25%, 50%, or 75% and for a 1:1 methane/ethylene mixture. In all cases the same product mass peaks appear (at least up to $n \leq 10$). Figure 10 compares mass spectra of products from ethane with those for the 1:1 CH_4/C_2H_6 mixture, normalized to the reactant mass peak. This shows that the only effect of adding methane is to increase the $n = 3$ peak (and of course $n = 1$); the intensity of all the other peaks is accounted for by the ethane content of the reactant gas. Thus, except for the enhanced yield of C_3H_m, in these mixtures methane appears to behave qualitatively like an inert gas with respect to forming higher hydrocarbons.

We also carried out runs with 1:1 mixtures of CD_4 and ethane, to examine further the apparent inertness of methane. The mass spectra exhibit many additional peaks (Figures 4 and 5), showing deuteration of the higher hydrocarbon products. This reveals that D atoms derived from methane do indeed contribute, but cannot show the extent to which this is via carbon-containing radicals, such as CD_3 or CD. Scrutiny of the C1 and C2 regions for the parent species (Figure 7b), as well as the mass spectra of the products, indicates that many of the peaks involving deuterium can be plausibly attributed to participation of CD and to a lesser extent CD_2 or CD_3 radicals. Comparison with the results for pure ethane (Figure 4) brings out another feature. Since the C_nH peaks (37, 49, 61, ...) can come only from the

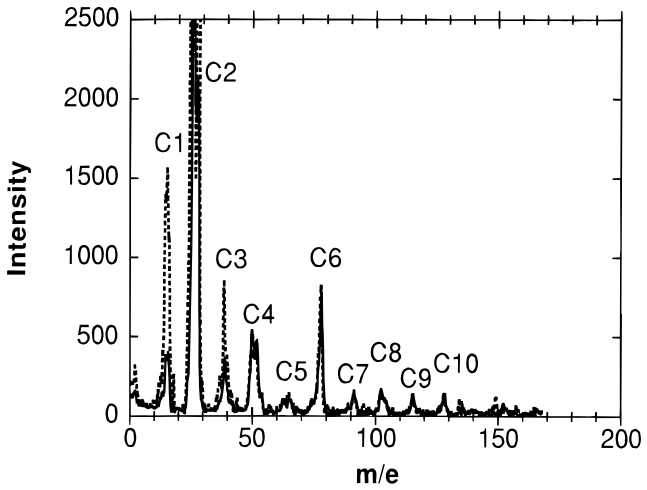

Figure 10. Comparison of mass spectra of reactants and products for C_2H_6 (full curves) and for 1:1 CH_4/C_2H_6 mixture (dashed curves, normalized to full for C2 peak) reacting in a Ni nozzle at 60 Torr and 1045 °C.

ethane component, comparison with the C_n peak indicates that methane contributes to the latter about as much as ethane does for $n = 3$, but considerably less for $n = 4$ and practically not at all for $n = 5$. However, in the $n = 6$ region (Figure 5), the mixture displays a prominent mass peak at 79, and sizable peaks at 80 and 81 showing substantial contributions from methane, although the overall yield of benzene is less for the mixture than for pure ethane.

4. Discussion

A few general aspects of the reaction mechanism can be inferred from our results, in the context of other work. The catalytic metal surface clearly has an essential role, in supplying precursor hydrocarbon radicals and hydrogen atoms. However, at ~800−1000 °C these would rapidly degrade to carbon and hydrogen unless liberated into the gas phase. The desorption is probably appreciably fostered by the strong flow of the reactant gas as well as the surface temperature. Much or most of the association reactions producing higher hydrocarbons may occur during the supersonic expansion. The effectiveness of the minimalist "button" version of the nozzle indeed suggests it is sufficient for the catalytic process to occur only near the exit aperture, thereby allowing the renascent products or reaction intermediates to promptly undergo free jet expansion.

The key reactions forming the higher hydrocarbons involve addition of radicals to unsaturated bonds. Recent model calculations for association reactions in hydrocarbon pyrolysis and flames have emphasized the role of chemically activated association and isomerization in overcoming entropic inhibitions, particularly for benzene formation.[23] A supersonic expansion can also promote association reactions, as in the formation of fullerenes,[24] since it greatly weakens entropic inhibition of molecular combination by markedly lowering the translational temperature for relative motion of the molecules.

The complexities of heterogeneous catalysis coupled with supersonic flow inhibit discussion of specific chemical steps. However, we note some aspects that seem akin to homogeneous gas-phase pyrolysis of hydrocarbons (in the absence of a catalyst). The resemblance we find between ethane and ethylene in forming higher hydrocarbons is consistent with the classic Rice−Herzfeld mechanism for pyrolysis of ethane, in which a chain carried by methyl radicals and H atoms converts ethane to ethylene.[12] This would also imply that ethylene should give larger yields, as observed. The fact that pure methane fails to produce higher hydrocarbons in our experiments is consistent with the pyrolysis of methane,[25] which gives only a minuscule yield of ethane and unsaturated products at short times.

A catalytic nozzle can produce large yields from association reactions whenever precursor radicals and unsaturated bonds are made available early in the expansion. Many other combinations of metal surfaces and gaseous reactants invite study, and pressure, temperature, and contact time within the nozzle can be varied widely. Kindred studies of surface reactions with flowing gas may also become feasible, by virtue of the recent development of techniques capable of monitoring surface species during reactions at high pressures and temperatures.[26]

Acknowledgment. We thank Benjamin Abbott, Theodore Hong, Dr. Alkwin Slenczka, and Dr. Bretislav Friedrich for aid with various aspects of the experiments. We have enjoyed instructive discussions with Dr. Christopher Nagel (Molten Metal Technology), with Dr. Anthony Dean (Exxon Corporate Science), and with Professors Sylvia Ceyer (MIT), Cynthia Friend (Harvard), Jack Lunsford (Texas A & M), and Gabor Somerjai (Berkeley). Major support for this work was provided by Molten Metal Technology; L.S. is grateful also to Boston College for a Dissertation Fellowship, and D.H. to the Miller Institute for Basic Science for a Visiting Professorship at Berkeley.

References and Notes

(1) Langmuir, I. *J. Am. Chem. Soc.* **1912**, *34*, 1310.
(2) Lunsford, J. H. *Langmuir* **1989**, *5*, 12.
(3) Fenn, J. B. *Annu. Rev. Phys. Chem.* **1996**, *47*, 1.
(4) Leopold, K. R.; Fraser, G. T.; Novick, S. E.; Klemperer, W. *Chem. Rev.* **1994**, *94*, 1807. See also: *Faraday Discuss. Chem. Soc.* **1994**, *97*.
(5) Castleman, A. W., Jr.; Wei, S. *Annu. Rev. Phys. Chem.* **1994**, *45*, 685.
(6) Larsen, R. A.; Neoh, S. K.; Herschbach, D. R. *Rev. Sci. Instrum.* **1974**, *45*, 1511. Mariella, R. P., Jr.; Neoh, S. K.; Herschbach, D. R.; Klemperer, W. *J. Chem. Phys.* **1977**, *67*, 2981.
(7) Kim, S. K.; Lee, W.; Herschbach, D. *J. Phys. Chem.* **1996**, *100*, 7933.
(8) Kohn, D. W.; Clauberg, H.; Chen, P. *Rev. Sci Instrum.* **1992**, *63*, 4003.
(9) See, for example: Weida, M. J.; Nesbitt, D. J. *J. Chem. Phys.* **1996**, *105*, 10310. Ohshima, Y.; Endo, Y. *J. Mol. Spectrosc.* **1989**, *153*, 627 and references therein.
(10) Kroto, H. W.; Heath, J. R.; O'Brien, S. C.; Curl, R. F.; Smalley, R. E. *Nature* **1985**, *318*, 162 and references therein.
(11) Shebaro, L.; Abbott, B.; Hong, T.; Slenczka, A.; Friedrich, B.; Herschbach, D. *Chem. Phys. Lett.* **1997**, *271*, 73.
(12) Benson, S. *Thermochemical Kinetics*, 2nd ed.; Wiley: New York, 1976; pp 343−363.
(13) Ceyer, S. T. *Science* **1990**, *249*, 133 and references therein.
(14) Beebe, T. P., Jr.; Goodman, D. W.; Kay, B. D.; Yates, J. T. *J. Chem. Phys.* **1987**, *87*, 2305. Sault, A. G.; Goodman, D. W. *J. Chem. Phys.* **1988**, *88*, 7232.
(15) Schmidt, L. D.; Huff, M. *Catalytic Oxidation*; Sheldon, R. A., Vam Santen, R. A., Eds.; World Scientific: Singapore, 1995; pp 93−117.
(16) Stanton, J. F.; DePinto, J. T.; Seburg, R. A.; Hodges, J. A.; McMahon, R. J. *J. Am. Chem. Soc.* **1997**, *119*, 429.
(17) McCarthy, M. C.; Travers, M. J.; Kovacs, A.; Chen, W.; Novick, S. E.; Gottlieb, C. A.; Thaddeus, P. *Science* **1997**, *275*, 518 and references therein.
(18) Kaiser, R. I.; Ochsenfeld, C.; Head-Gordan, M.; Lee, Y. T. Lee; Suits, A. G. *Science* **1996**, *274*, 1508.
(19) Shebaro, L. Ph.D. Dissertation, Boston College, 1996.
(20) Morter, C. L.; Farhat, S. K.; Adamson, J. D.; Glass, G. P.; Curl, R. F. *J. Phys. Chem.* **1994**, *98*, 7029.
(21) Cornu, A.; Massot, R. *Compilation of Mass Spectral Data*, 2nd ed.; Heyden & Son: London, 1975; Vols. 1 and 2.
(22) Alkemade, U.; Homann, K. H. *Z. Phys. Chem. (Munich)* **1989**, *161*, 19.
(23) Westmoreland, P. R.; Dean, A. M.; Howard, J. B.; Longwell, J. P. *J. Phys. Chem.* **1989**, *93*, 8171. Bozzelli, J. W.; Dean, A. M. *J. Phys. Chem.* **1993**, *97*, 4427.
(24) Goroff, N. S. *Acc. Chem. Res.* **1996**, *29*, 77.
(25) Dean, A. M. *J. Phys. Chem.* **1990**, *94*, 1432.
(26) Somorjai, G. A. *Z. Phys. Chem.* **1996**, *197*, 1.